LWT - Food Science and Technology 137 (2021) 110385

Contents lists available at ScienceDirect

LWT

journal homepage: www.elsevier.com/locate/lwt

Heat inactivation of thermolabile polygalacturonase down to single molecule level. Systematic investigation and molecular modeling

Ana Serrano-Martínez [a], Iuliana Aprodu [b], Iuliana Banu [b], Carmen Lucas-Abellán [a], Pilar Hernández Sánchez [a], Lucía Guardiola [a], Estrella Núñez-Delicado [a], Vicente M. Gómez-López [c,*]

[a] Molecular Recognition and Encapsulation Research Group (REM), Health Sciences Department, Universidad Católica de Murcia (UCAM), Campus de los Jerónimos 135, Guadalupe, 30107, Spain
[b] Dunărea de Jos University of Galati, Faculty of Food Science and Engineering, Domnească Street 111, 800201 Galati, Romania
[c] Cátedra Alimentos para la Salud, Universidad Católica de Murcia (UCAM), Campus de los Jerónimos 135, Guadalupe 30107, Murcia, Spain

ARTICLE INFO

Keywords:
Enzyme inactivation
Food quality
Thermal treatment
Structure-function
In silico

ABSTRACT

Polygalacturonase is an important enzyme related to quality of fruits and vegetables that it is usually inactivated by heat. This research aimed to determine the structural changes associated with the thermal inactivation of thermolabile polygalacturonase (PG2), which were studied using molecular modeling and by measuring the free sulfhydryl and intrinsic fluorescence changes. The inactivation followed a first-order kinetics during 5 min of heating (50–80 °C). The *in silico* investigation at single molecule level revealed that the temperature increase up to 80 °C affected the overall conformation of the catalytic site. When compared to the native enzyme, important changes of the surface available to the solvent of two catalytic amino acids, Asp^{202} and His^{223}, were noticed at 70 °C (−27.7% and +108.6%, respectively). Further temperature increase up to 80 °C disrupted the hydrogen bonds connecting the amino acids within the catalytic site (His^{223}–Asp^{201}) and between the catalytic and binding site (Asp^{201}-Lys^{258}). Intrinsic fluorescence changes revealed perturbation of the tertiary structure and were in line with an all-or-none process. The evolution of free sulfhydryl indicated reaction of the Cys^{109} residue. The most important event in the thermal inactivation of PG2 is likely the narrowing of the access to the catalytic site.

1. Introduction

Polygalacturonase (PG) (EC 3.2.1.15) is one of the most important enzymes related to quality of fruits, vegetables and their products, because it plays a major role in the degradation of pectin. This enzyme hydrolyzes the α-glycosidic bonds in the homogalacturonan region of pectin (van Pouderoyen et al., 2003).

The activity of this enzyme is sometimes wanted and in some cases must be avoided, depending on specific technological goals. It is desirable in cases when industry wants to improve juice clarification or enhance juice extraction. On the other hand, the inactivation of this enzyme is carried out to preserve fruit texture and juice cloudiness, or to prevent consistency loss in pastes and purées of plant sources (Duvetter et al., 2009; Jolie et al., 2012).

Thermal treatments have been used for many years for the inactivation of PG. A comprehensive review about thermal stability of this enzyme from fruits and vegetables is provided by Duvetter et al. (2009). In spite of the importance of this enzyme and the long lasting use of heat to inactivate it, there is a lack of information about the structural changes associated with its thermal inactivation. Many other important food related enzymes have shared this feature until recent times. The use of new tools for modeling, measuring and analyzing the structural changes of proteins promoted by environmental factors such as pH and temperature have made possible to fill gaps and unveil how enzymes such as polyphenol oxidase (Ioniță et al., 2014), pectinmethylesterase (Nistor et al., 2014) and peroxidase (Stănciuc et al., 2015) are inactivated by heat. While the structure-activity relationship in PG has been studied to describe the effect of pH (Aminzadeh et al., 2010) and of processing through an emerging technology (Pellicer et al., 2019), the literature lacks the equivalent information about the inactivation of this relevant enzyme by the method most commonly applied worldwide to inactivate it.

* Corresponding author.,.
E-mail address: vmgomez@ucam.edu (V.M. Gómez-López).

https://doi.org/10.1016/j.lwt.2020.110385
Received 20 July 2020; Received in revised form 3 September 2020; Accepted 10 October 2020
Available online 12 October 2020

It is widely accepted that PG has several isoforms, generally two, a thermolabile and a thermoresistant form (Duvetter et al., 2009). This has been evidenced in several studies as compiled by Duvetter et al. (2009), including the widely studied PG from tomato products (Anthon et al., 2002) and PG from the same commercial source as in case of the present research (Ma et al., 2015). The large difference in thermostability of the two isoforms allows studying their thermal inactivation independently (Anthon et al., 2002). Two proteins with polygalacturonase activity and different thermal resistance have been identified in PG extracts from *Aspergillus flavus*. There are important differences in primary structure between the thermoresistant and the thermolabile PG isoenzymes, which can be deducted taken into account their respective molecular weights (216.08 vs 76.27 kDa) and residue counts (670 vs 2016) (van Pouderoyen et al., 2003; Van Santen et al., 1999). They share a sequence similarity of 60% (van Pouderoyen et al., 2003). In the present study, we focused on the thermolabile isoenzyme, called PG2; which consists of a single polypeptide chain with a predominant β-sheet secondary structure folded as a β-helix (Van Santen et al., 1999).

Therefore, the aim of this research was to provide insight on the structural changes associated to the thermal inactivation of PG2, which was pursued by means of fluorescence spectroscopy techniques and measuring free sulfhydryl of the enzyme heat treated at different temperatures. Further atomic level details of the events responsible for enzyme inactivation were provided after performing molecular dynamics simulations.

2. Materials and methods

2.1. Materials

Polygalacturonase from *Aspergillus niger*, polygaracturonic acid, cyanoacetamide, TRIS, HCl, 1-anilino-8-naphthalenesulfonate (ANS), KI and borate buffer were purchased from Sigma-Aldrich (St. Louis, USA) and acetate buffer from Scharlau (Scharlab, Barcelona, Spain).

2.2. Heat treatment

A 0.5 mg/mL (13.81 μM) suspension of the enzyme in acetate buffer pH 4, 50 mM, was prepared and placed in test tubes which were immersed in a water bath for 10 min at pre-set temperatures (25, 50, 60, 70 and 80 °C). In order to determine the kinetics of inactivation, samples were withdrawn every minute to measure residual enzymatic activity.

For the study of the structural changes of the enzyme through fluorescence spectroscopy technique, the thermal treatments were carried for only 5 min because this time was enough to selectively inactivate the thermolabile PG. After the thermal treatment, the samples were rapidly cooled to 25 °C, such as to avoid further denaturation events.

All measurements were performed in triplicate and mean values are reported.

2.3. Enzymatic activity

The PG activity was assayed according to Aguiló-Aguayo et al. (2008) by mixing 100 μl of enzyme suspension with 300 μl of 0.2% (w/v) polygaracturonic acid in acetate buffer of pH 4.0. The mixture was incubated for 10 min at 35 °C in a water bath, and then the reaction was stopped by adding two ml of 100 mM borate buffer of pH 9.0 and 400 μl of 1% (w/v) (1.19 mM) cyanoacetamide, followed by boiling for 10 min. After cooling down, the absorbance was measured in a spectrophotometer (UV–Vis spectrophotometer, Shimadzu model UV-1603, Japan) at 276 nm and 22 °C. Simultaneously, a blank was prepared with the same reagents but without enzyme.

2.4. Tryptophan steady-state fluorescence

Intrinsic fluorescence of heat treated enzyme was measured at 25 °C in a quartz cuvette of 1 cm optical path length, using a spectrofluorimeter RF-Shimadzu (Japan). The excitation wavelength of 293 nm was used and fluorescence emission was collected between 300 and 450 nm. Fluorescence data were analyzed by emission spectra, center of spectral mass, parameter A and phase diagram.

The center of spectral mass (Ferrão-Gonzales et al., 2000) was calculated according to the following equation:

$$\lambda_{av} = \sum \lambda\, F(\lambda) \Big/ \sum F(\lambda)$$

where λ_{av} is the center of mass (nm) and F(λ) is the fluorescence at wavelength λ.

Parameter A (Turoverov et al., 1976) was obtained by the following equation:

$$parameter\ A = \left(\frac{I_{320}}{I_{365}}\right)_{293}$$

where I_{320} and I_{365} are fluorescence intensities at emission wavelengths of 320 and 365 nm, respectively, for an excitation wavelength set to 293 nm.

The phase diagram was elaborated according to the following equation:

$$I(\lambda_{365}) = a + b\ I(\lambda_{320})$$

where a and b are the intercept and the slope of the plot respectively (Kuznetsova et al., 2004).

2.5. Free sulfhydryls concentration

The determination of free sulfhydryl content was carried out according to Ellman (1959) as adapted by Siddique et al. (2017), but with an enzyme concentration of 0.5 mg/mL (13.81 μM). In brief, 2.75 mL of enzyme solution was mixed with 0.25 mL of a 1 g/L (2.52 mM) of Ellman's reagent in 50 mM Tris-HCl buffer. After 30 min of incubation in darkness at room temperature, the absorbance at 412 nm was measured and the concentration of free sulfhydryls was calculated according to Beveridge et al. (1974).

2.6. Molecular modeling

Single molecule level investigations on thermal dependent behaviour of PG2 were performed by employing the molecular mechanics and molecular dynamics techniques. The X-ray crystallographic model of endopolygalacturonase from *A. niger* (PDB ID 1CZF) solved by Van Santen et al. (1999) was taken from the Brookhaven Protein Data Bank. The first steps of the *in silico* test involved the use of molecular mechanics to optimize the refined 3D model consisting of a single PG2 molecule. A sequence of two algorithms (steepest descent and limited-memory Broyden−Fletcher−Goldfarb−Shanno) was used for energy minimization *in vacuum* and after protein solvation using single point charge explicit water molecules. The system consisted of 71,343 atoms, including 22,742 water molecules. After elimination of eventual geometry distortions and of strong repulsive non-bonded contacts, the solvated protein was heated up to 25, 50, 60, 70 and 80 °C by coupling each component of the system to a Berendsen thermostat. The models heated at different temperatures were then equilibrated for 2000 ps by means of molecular dynamics steps to soften eventual temperature and energy oscillation. All energy minimization and molecular dynamics simulations were carried out using GROMACS code (version 5.1.1.; Groningen University, The Netherlands), and gromos43a1 force field (Abraham et al., 2015; van der Spoel et al., 2005). The molecular dynamics steps were run in parallelization conditions on the High

Performance Computer System (HPC) from *Dunarea de Jos* University of Galati, Romania using Intel E5 2680 v3, 12-cores, 2.5 GHz. The equilibrated protein models were analyzed in terms of energy, structural and conformation particularities using dedicated Gromacs, PDBsum (Laskowski, 2009), PDBePISA (Krissinel & Henrick, 2007) (The European Bioinformatics Institute, Cambridge, UK) and Visual Molecular Dynamics (VMD) (Humphrey et al., 1996) tools.

3. Results and discussion

3.1. Kinetics of polygalacturonase inactivation

The kinetics of PG2 inactivation up to 5 min of heating is shown in Fig. 1. Inactivation experiments were conducted up to 10 min; however, the inactivation followed first-order kinetics only during the first 5 min of heating. This finding is characteristic of poligalacturonase preparations and it is a consequence of the co-existence of two isoforms with different thermostability. During the first 5 min of heating at 50–80 °C only the thermolabile form is affected. This result is in line with a previous report about the thermal inactivaction of PG from the same source used that the one used in the current study (Ma et al., 2015).

The inactivation of PG2 was very small at 50 °C, which justifies the use of this temperature as a starting point to study its thermal inactivation. It has been reported that temperatures of 25, 30 and 40 °C has no effect up to 2 h on the thermostability of PG2 from *A. niger* (Hendges et al., 2011). The rate of thermal inactivation of PG2 activity increased with temperature (Table 1) and its enzymatic activity decreased by 85% after 5 min of heating at 80 °C. The activation energy was calculated as 109 kJ/mol (R^2 of 0.93).

3.2. Analysis of thermally induced behaviour of PG2 at single molecule level

The *in silico* approach was employed to look for the atomic level events standing behind the thermal behaviour of PG2. In agreement with the experimental conditions, the X-ray crystallographic model of PG2 from *A. niger* was heated and equilibrated at different temperatures ranging from 25 to 80 °C. Regardless of the simulated temperature, the structure of PG2 is well packed into a right-handed parallel β-helix. Taking into account that the proteins rich in β-sheets are stable against thermal treatment (Aprodu et al., 2013), no significant impact on the overall enzyme secondary structure was noticed with the temperature increase. Some β-sheets topology changes were noticed at temperature over 60 °C, consisting in the decrease of the number of connections between strands, but the four parallel β-sheets preserved the ability to shield the hydrophobic core of the enzyme. The most important change which might impact the enzyme activity when raising the temperature from 60 °C to 80 °C refers to the shrinkage of the β-sheet strand with major role in substrate binding, from Thr^{247}-Ile^{260} to Asn^{253}-Thr^{259}.

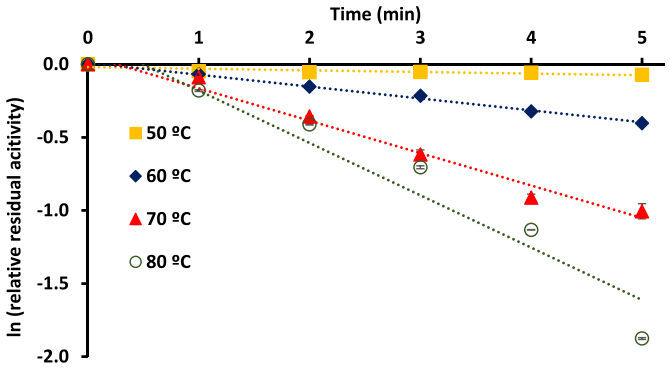

Fig. 1. Kinetics of thermal inactivation of polygalacturonase 2 at different temperatures. Bars represent standard deviations.

Table 1
Inactivation rate of polygalacturonase 2 during heating at different temperatures for 5 min.

Temperature (°C)	Inactivation rate (1/min)	R^2
50	0.0111	0.71
60	0.0813	1.00
70	0.2217	0.98
80	0.3581	0.93

Moreover, the Asn^{199}-Asp^{202} sequence, which guests two residues potentially responsible for substrate hydrolysis (Van Santen et al., 1999), belonging to a strand of the parallel β-sheet from enzyme secondary structure at 60 °C, suffered an important transition towards a beta turn motif when heating at 80 °C.

Although the PG2 volume did not change within the temperature range considered in the study, a slight increase of the hydrophobic surface available to the solvent (and of total surface was observed at 70 °C, followed by a decrease at even higher temperature (Table 2). These results suggest small structural rearrangements at high temperature, consisting on protein refolding on a different pattern compared to the native protein. The dynamics of the hydrogen bonding network appeared to be involved in supporting these molecular events. When increasing the temperature up to 80 °C, a gradual decrease, from 557 to 514, of the HBs connecting the amino acids on the protein surface by the water molecule was noticed (Table 2), because of the changes occurring in protein surface.

Although the well packed structure of PG2 was rather well conserved over the entire tested temperature range, important changes were noticed when exploring the active site. As hypothesised by Van Santen et al. (1999), who performed site directed mutagenesis to assess the importance of different residues for enzyme activity, Asp^{180}, Asp^{201}, Asp^{202} and His^{223} might be directly involved in substrate hydrolysis, while Arg^{256} and Lys^{258} might be responsible for substrate binding. These negatively charged residues belong to the PB1 parallel β-sheet which forms the bottom of the ~8 E wide cleft (Van Santen et al., 1999). This large cleft is delimited by two extensions consisting of the longest loops from the protein structure. The first loop is located near the C terminal side of the T1 turns connecting the PB1 and PB2 β-sheets, and the second loop near the N terminal side of the T2 turns connecting the PB3 and PB1 β-sheets of the right-handed parallel β-helical structure. The catalytic site containing cleft is double opened (Fig. 2) and therefore suitable to accommodate the unbranched polygalacturonan chains. The heat induced structural changes affected the opening of the enzyme pocket; the two loops gradually approached each other (Fig. 2), most probably disturbing the substrate recognition and binding by the enzyme and making more difficult its hydrolysis by the catalytic site. The smallest distance between the two loops delimiting the cavity that accommodates the catalytic site decreased from 14.16 Å to 8.38 Å when increasing the temperature from 25 °C to 80 °C (Fig. 2). These observations are in good agreement with the experimental results, explaining the more rapid inactivation of PG2 at higher temperature (Fig. 1).

In order to estimate the impact of the thermal treatment on the local conformation of the active site, the exposure and the distance between the center of mass of Asp^{180}, Asp^{201}, Asp^{202} and His^{223} of the catalytic tetrade were assessed using the spatial coordinates of each atom of the amino acids (Table 3). Moreover, taking into account the important role of HBs in stabilising the active site of enzymes, the hydrogen bonding network involving the catalytic amino acids was also followed.

Important changes in the exposure of different catalytic amino acids to the solvent were noticed when heating the enzyme from 25 °C to 80 °C. In particular, about 81% of Asp^{201} surface exposed to the solvent at 25 °C got buried at 50 °C, resulting in significant change of the relative position in respect to His^{223} (the Asp^{201} - His^{223} distance decreased from 5.54 Å to 5.14 Å). Anyway, the most important events suggesting severe perturbation of the catalytic tetrade microenvironment were noticed at

Table 2
Structure and energy details of polygalacturonase 2 under thermal treatment.

	Temperature				
	25 °C	50 °C	60 °C	70 °C	80 °C
Overall structure descriptors					
Volume, nm^3	51.82 ± 0.87	51.70 ± 0.94	51.61 ± 1.28	51.42 ± 1.36	51.12 ± 1.61
HSAS, nm^2	69.38 ± 0.87	69.67 ± 1.61	70.26 ± 0.99	72.65 ± 1.50	70.08 ± 1.23
Total surface, nm^2	136.86 ± 1.22	137.18 ± 2.19	136.21 ± 1.52	140.07 ± 2.12	137.56 ± 1.84
HBs within the protein	257 ± 10	255 ± 8	261 ± 5	246 ± 5	250 ± 7
HBs between protein and water	557 ± 11	539 ± 11	513 ± 12	521 ± 10	514 ± 17
Energy descriptors					
Potential energy, $kJ{\cdot}mol^{-1}$	$-1000.35{\cdot}10^3$ ±972.26	$-959.00{\cdot}10^3$ ±1130.24	$-943.68{\cdot}10^3$ ±637.82	$-928.29{\cdot}10^3$ ±1118.48	$-913.29{\cdot}10^3$ ±955.43
Total energy, $kJ{\cdot}mol^{-1}$	$-735.21{\cdot}10^3$ ±904.48	$-671.63{\cdot}10^3$ ±1040.74	$-647.34{\cdot}10^3$ ±596.99	$-623.02{\cdot}10^3$ ±866.00	$-599.13{\cdot}10^3$ ±922.84

HBs – hydrogen bonds; HSAS – hydrophobic surface available to the solvent.

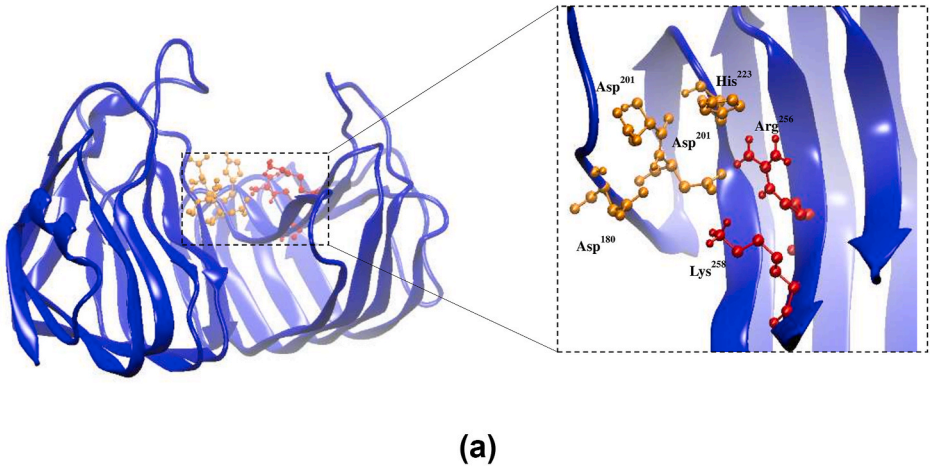

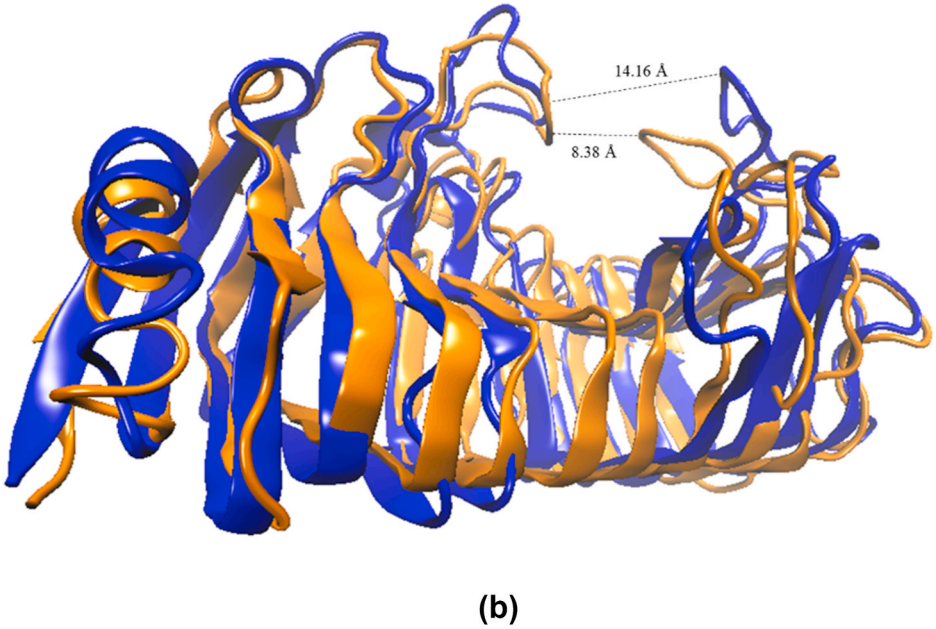

Fig. 2. (a) The three-dimensional model of polygalacturonase (PG2) equilibrated at 25 °C. In the inset are presented atomic details on the binding (red; Arg^{256} and Lys^{258}) and catalytic site (yellow; Asp^{180}, Asp^{201}, Asp^{202} and His^{223}) of PG2. The overall folding of PG2 is represented in blue in Catmull-Rom NewCartoon style, and the residues of the active site are represented in CPK style. (b) Differences in the molecular models observed by superimposing the PG2 structures equilibrated at 25 °C (dark, blue) and 80 °C (clear, orange). The access of the substrate to the catalytic site located at the bottom of PG2 cleft formed by the loop regions T1 (loop located on the right side of cleft) and T3 (loop located on the left side of the cleft) which got closer together at high temperature. Images are prepared using Visual Molecular Dynamics (VMD) software (Humphrey et al., 1996). (For interpretation of the references to colour in this figure legend, the reader is referred to the Web version of this article.)

temperature over 60 °C. The 3.2 Å long HB bridging the main chain of Asp^{202} by the side chain of Asp^{180} is broken at 60 °C, as a consequence of changing of the relative position of the two catalytic residues, causing the increase of the distance between their center of mass (Table 3). Furthermore, the disruption of the HB between the side chains of Asp^{202} and Arg^{256} involved in stabilising the position of the catalytic site in

Table 3
Atomic level details on the catalytic site of polygalacturonase subjected to thermal treatment.

Descriptor		Temperature, °C				
		25	50	60	70	80
ASA, Å^2	Asp^{180}	40.24	35.65	34.4	36.07	21.56
	Asp^{201}	28.92	5.54	32	26	10.92
	Asp^{202}	11.84	10.23	13.78	8.56	13.74
	His^{223}	30.3	33.95	16.43	63.2	25.54
Δ^sG, kcal/mol	Asp^{180}	−0.52	−0.49	−0.3	−0.28	−0.3
	Asp^{201}	−0.37	−0.04	−0.43	−0.04	−0.08
	Asp^{202}	−0.19	−0.17	−0.18	0.07	−0.18
	His^{223}	−0.72	−0.41	−0.26	0.06	−0.55
Distances between catalytic amino acids, Å	Asp^{180} - Asp^{201}	4.98	4.87	4.87	4.86	5.05
	Asp^{180} - Asp^{202}	5.22	5.28	5.41	4.90	4.87
	Asp^{180} - His^{223}	9.05	8.76	8.87	9.13	8.54
	Asp^{201} - Asp^{202}	4.74	4.76	4.56	4.86	4.78
	Asp^{201} - His^{223}	5.54	5.14	5.21	5.96	5.54
	Asp^{202} - His^{223}	4.76	4.68	4.40	5.08	4.29
No. of HBs and amino acids* involved in HBs with the catalytic amino acids	Asp^{180}	2 - Ala^{151}, **Asp^{202}**	2 - Ala^{151}, **Asp^{202}**	1 - Ala^{151}	2 - Ala^{151}, Asn^{178}	1 - Ala^{151}
	Asp^{201}	5 - Thr^{179}, Asn^{199}, **His^{223}**	4 - Thr^{179}, Asn^{199}, **His^{223}**	4 - Thr^{179}, Asn^{199}, **His^{223}**	5 - Asn^{178}, Thr^{179}, Asn^{199}, **His^{223}**	3 - Asn^{178}, Thr^{179}
	Asp^{202}	3 - **Asp^{180}**, Ser^{226}, *Arg^{256}*	4 - **Asp^{180}**, Ala^{181}, Gly^{224}, *Arg^{256}*	2 - Ala^{181}, Ser^{226}	3 - Ala^{181}, Ser^{226}, *Lys^{258}*	1 - Ser^{226}
	His^{223}	2 - **Asp^{201}**, Cys^{203}	3 - **Asp^{201}**, Cys^{203}, Asn^{253}	2 - **Asp^{201}**, Cys^{203}	3 - **Asp^{201}**, Cys^{203}, Asn^{253}	3 - Asn^{199}, Asn^{253}

ASA – accessible surface area; Δ^sG – hydrophobic interaction with the solvent. * Catalytic residues are emphasized in bold, while the amino acids from the binding site are in italic.

respect to the binding site of PG2 at temperature over 50 °C was attributed to the twisting motion of Asp^{202} side chain around the protein backbone. Significant lower exposure to the solvent of Asp^{202} was registered at further temperature increase up to 70 °C, accompanied by the increase of the hydrophobic interaction energy up to positive values (Δ^sG increased from −0.18 kcal/mol at 60 °C up to 0.07 kcal/mol at 70 °C), therefore suggesting that no spontaneous contact between the amino acid and water molecules is favored. Under these environmental conditions, the Asp^{202} became available for establishing new HB with the Lys^{258}, which is the second amino acid nominated for being involved in substrate binding. On the other hand, the exposure of His^{223} at 70 °C increased by 108.6% compared to the model equilibrated at 25 °C. The conformation of the catalytic site was affected by the thermal movement of His^{223} toward the surface of PG2 cavity. Important increase of the distance between His^{223} and the other three catalytic amino acids was noticed when increasing the temperature from 60 to 70 °C (Table 3). Finally, when heating the enzyme up to 80 °C, the His^{223} got buried by the β27 strand of the PB1 β-sheet (Van Santen et al., 1999), resulting in the rupture of the HB between this residue and Asp^{201}.

Close analysis of the HB networking indicated that only three bridges involved in stabilising the conformation of the catalytic site were conserved over the entire tested temperature range. At 25 °C Asp^{201} is bridged to the Thr^{179} residue through three HBs, out of which one connects the side chains of the two residues and is broken at 50 °C, whereas the others are main chain – side chain type and are stable up to 80 °C. In addition, the main chain-main chain type HB connecting the Asp^{180} by Ala^{151} was well conserved (Table 3), regardless of the thermal treatment applied to the PG2.

3.3. Intrinsic fluorescence

The intrinsic fluorescence properties were used to follow the heat induced changes in protein structure. Fig. 3a shows the effect of different heating temperatures on the tryptophan intrinsic fluorescence of PG2. This molecule has seven tryptophan (Trp) residues, located in positions 85, 114, 115, 196, 213, 337 and 339. Out of this residues, Trp^{114} is completely buried within the hydrophobic core of the native enzyme, whereas others are either partially buried, such as Trp^{85}, Trp^{115}, Trp^{337} and Trp^{339} with surfaces exposed to the solvent (SAS) ranging from 13.72 Å^2 to 47.52 Å^2, or almost completely exposed to the solvent, such as Trp^{196} and Trp^{213} with SAS of 99.77 Å^2 and 98.46 Å^2, respectively. Analyzing the results presented in Fig. 3a one can see that the fluorescence intensity was maximal for the native protein and decreased progressively with the increment of the temperature of the treatment. These results provide evidence that heat disturbs the tertiary structure of the protein. The applied analytical parameters preferentially excite Trp residues, which have a high quantum yield under the hydrophobic conditions existing in the core of the native protein and reduced quantum yielded when exposed to the hydrophilic microenvironment of the buffer that suspends it (Dumitraşcu et al., 2016). The trend registered in the fluorescent properties of PG2 subjected to increasing temperature is in agreement with the results reported by Pellicer et al. (2019) when performing inactivation of PG by pulsed light. On the other hand, the ultrasound treatment promoted a higher fluorescence of the protein (Ma et al., 2015).

Further evidence of disturbed tertiary structure of PG2 was provided by the changes of center of spectral mass and parameter A (Fig. 3b and c). The red shift of λ_{max} corresponding to the maximum fluorescence intensity is another evidence of enzyme conformational changes, but small shifts are difficult to differentiate. This inconvenient is coped by using the center of spectral mass, which allows quantifying spectral shifts more accurately than the wavelength of maximum emission (Royer & Weber, 1986) and by parameter A, which can easily detect spectral shifts of less than 1 nm (Turoverov et al., 1976). Fig. 3b shows that increasing temperature during inactivation caused red shifts in the center of spectral mass, suggesting the gradual change of the polarity of the Trp environment, due to the movement of these residues towards the proteins surface. These findings are in good agreement with the trend

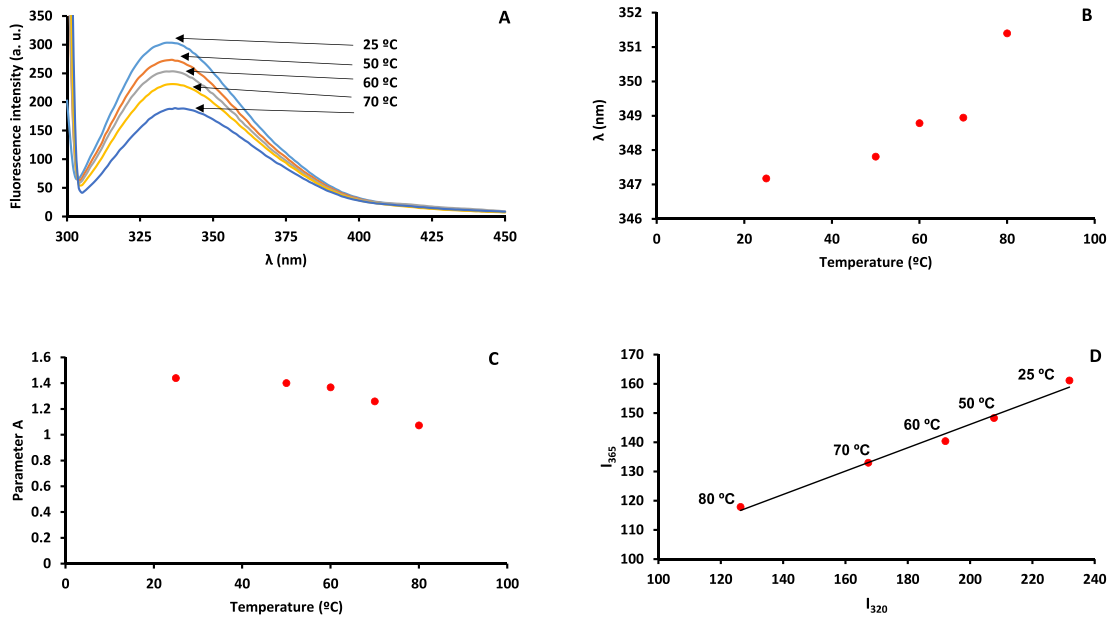

Fig. 3. Changes in intrinsic fluorescence of polygalacturonase 2 at different thermal treatment temperatures. A. Emission spectra. B. Center of spectral mass. C. Parameter A. D. Phase diagram, I_{365} and I_{320}: fluorescence at 365 and 320 nm respectively.

registered for parameter A (Fig. 3c), showing important conformational changes of PG2 structure at increasing temperature, which support the kinetics of PG2 inactivation.

Parameter A, as well as phase diagram, allows detecting intermediates of the enzymes during their inactivation. A phase diagram is linear if the inactivation is an all-or-none transition between two conformational states and exhibits different linear portions if the inactivation occurs in a sequence of multiple transitions between several intermediates (Kuznetsova et al., 2002). Results of the evolution of parameter A (Fig. 3c) and phase diagram (Fig. 3d) gave no evidence of intermediates, supporting the conclusion that the heat inactivation of PG2 is an all-or-none process. The same results have been reported for the inactivation of PG by pulsed light (Pellicer et al., 2019) and for other enzymes inactivated by heat such as glucose oxidase (Dumitraşcu et al., 2016).

3.4. Free sulfhydryls

The evolution of free sulfhydryl concentration of PG2 was evaluated after heating the protein at different temperatures. PG2 from *A. niger* has nine cysteine residues, out of which eight are involved in intramolecular disulfide bridges (Cys^{30}-Cys^{45}, Cys^{353}-Cys^{362}, Cys^{203}-Cys^{219} and Cys^{329}-Cys^{334}), and one, Cys^{109}, is free (Van Santen et al., 1999). The increase of free sulfhydryl during treatment is an indication of rupture of disulfide bridges. This was not observed during heating (Fig. 4), which leads to think that all disulfide bridges resisted the heating treatment. This result is in harmony with our *in silico* studies, which predicted a highly stable structure. The decrease of free sulfhydryl concentration can be attributed to cross-linking of PG2 molecules through the Cys^{109} residue. The change was linearly proportional to temperature (R^2 of 0.995). The detailed analysis of PG2 at single molecule level support these experimental observations, indicating that temperature increase from 25 °C to 80 °C resulted in gradual exposure of Cys^{109} residue, which became available for establishing intermolecular disulfide bonds.

4. Conclusion

The inactivation of PG2 by heat (50–80 °C) followed a first-order kinetics. The temperature increase from 25 °C to 80 °C caused the two loops delimiting the cavity that accommodate the catalytic site to get closer, the smallest distance between them decreasing by 40.82%. Narrowing the access of the polygalacturonan chains to the catalytic site of enzyme might affect substrate binding and hydrolysis. Additionally, changes in the tertiary structure of PG2 were promoted by heating as indicated by the decrease in intrinsic fluorescence and red shifts in the center of spectral mass and parameter A. The four disulfide bridges of the enzyme are preserved during heating and the Cys^{109} residue is prone to establish intermolecular disulfide bridges, as indicated by the decrease in free sulfhydryls. The phase diagram indicates that the heat inactivation of PG2 is an all-or-none process.

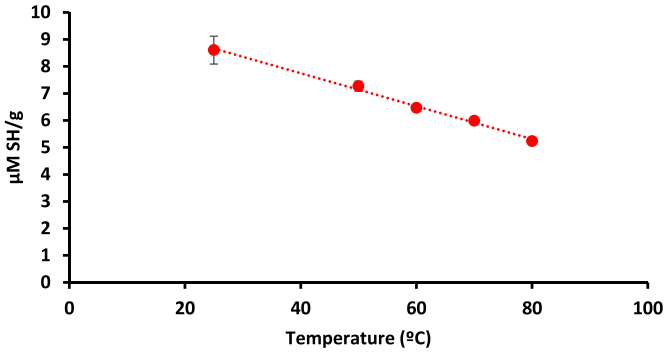

Fig. 4. Free sulfhydryl concentration of PG2 after heating for 5 min at different temperatures. Bars represent standard deviations.

CRediT authorship contribution statement

Ana Serrano-Martínez: Investigation. **Iuliana Aprodu:** Methodology, Software, Formal analysis, Writing - original draft, Writing - review & editing. **Iuliana Banu:** Software. **Carmen Lucas-Abellán:** Investigation. **Pilar Hernández Sánchez:** Investigation. **Lucía Guardiola:** Investigation. **Estrella Núñez-Delicado:** Writing - review & editing. **Vicente M. Gómez-López:** Conceptualization, Methodology, Supervision, Formal analysis, Writing - original draft, Writing - review & editing, Funding acquisition.

Declaration of competing interest

The authors declare that they have no known competing financial interests or personal relationships that could have appeared to influence the work reported in this paper.

Acknowledgments

This work was supported by Universidad Católica de Murcia, Spain, grant PMAFI/29/14.

References

Abraham, M. J., Murtola, T., Schulz, R., Páll, S., Smith, J. C., Hess, B., & Lindahl, E. (2015). GROMACS: High performance molecular simulations through multi-level parallelism from laptops to supercomputers. *Software, 1–2*, 19–25. https://doi.org/10.1016/j.softx.2015.06.001

Aguiló-Aguayo, I., Soliva-Fortuny, R., & Martín-Belloso, O. (2008). Comparative study on color, viscosity and related enzymes of tomato juice treated by high-intensity pulsed electric fields or heat. *European Food Research and Technology, 227*(2), 599–606. https://doi.org/10.1007/s00217-007-0761-2

Aminzadeh, S., Naderi-Manesh, H., Khajeh, K., Ranjbar, B., & Farrokhi, N. (2010). Characterization of acid-induced partially folded conformation resembling a molten globule state of polygalacturonase from a filamentous fungus *Tetracoccosporium* sp. *Applied Biochemistry and Biotechnology, 160*, 1921–1932. https://doi.org/10.1007/s12010-009-8723-8

Aprodu, I., Stănciuc, N., Banu, I., & Bahrim, G. (2013). Probing thermal behaviour of microbial transglutaminase with fluorescence and *in silico* methods. *Journal of the Science of Food and Agriculture, 93*, 794–802. https://doi.org/10.1002/jsfa.5799

Beveridge, T., Toma, S. J., & Nakai, S. (1974). Determination of SH- and SS-groups in some food proteins using Ellman's reagent. *Journal of Food Science, 39*, 49–51. https://doi.org/10.1111/j.1365-2621.1974.tb00984.x

Dumitraşcu, L., Stănciuc, N., Bahrim, G. E., Ciumac, A., & Aprodu, I. (2016). pH and heat-dependent behaviour of glucose oxidase down to single molecule level by combined fluorescence spectroscopy and molecular modelling. *Journal of the Science of Food and Agriculture, 96*, 1906–1914. https://doi.org/10.1002/jsfa.7296

Duvetter, T., Sila, D. N., Van Buggenhout, S., Jolie, R., Van Loey, A., & Hendrickx, M. (2009). Pectins in processed fruit and vegetables: Part I—stability and catalytic activity of pectinases. *Comprehensive Reviews in Food Science and Food Safety, 8*, 75–85. https://doi.org/10.1111/j.1541-4337.2009.00070.x

Ellman, G. L. (1959). Tissue sulfhydryl groups. *Archives of Biochemistry and Biophysics, 82*, 70–77. https://doi.org/10.1016/0003-9861(59)90090-6

Ferrão-Gonzales, A. D., Souto, S. O., Silva, J. L., & Foguel, D. (2000). The preaggregated state of an amyloidogenic protein: Hydrostatic pressure converts native transthyretin into the amyloidogenic state. *Proceedings of the National Academy of Sciences, 97*, 6445–6450. https://doi.org/10.1073/pnas.97.12.6445

Hendges, D. H., Montanari, Q., Malvessi, E., & da Silveira, M. M. (2011). Production and characterization of endo-polygalacturonase from *Aspergillus niger* in solid-state fermentation in double-surface bioreactor. *Brazilian Archives of Biology and Technology, 54*, 253–258. https://doi.org/10.1590/S1516-89132011000200005

Humphrey, W., Dalke, A., & Schulten, K. (1996). Vmd: Visual molecular dynamics. *Journal of Molecular Graphics, 14*(1), 33–38. https://doi.org/10.1016/0263-7855(96)00018-5

Ioniță, E., Aprodu, I., Stănciuc, N., Râpeanu, G., & Bahrim, G. (2014). Advances in structure–function relationships of tyrosinase from *Agaricus bisporus* – investigation on heat-induced conformational changes. *Food Chemistry, 156*, 129–136. https://doi.org/10.1016/j.foodchem.2014.01.089

Jolie, R. P., Christiaens, S., De Roeck, A., Fraeye, I., Houben, K., Van Buggenhout, S., … Hendrickx, M. E. (2012). Pectin conversions under high pressure: Implications for the structure-related quality characteristics of plant-based foods. *Trends in Food Science & Technology, 24*, 103–118. https://doi.org/10.1016/j.tifs.2011.11.003

Krissinel, E., & Henrick, K. (2007). Inference of macromolecular assemblies from crystalline state. *Journal of Molecular Biology, 372*, 774–797. https://doi.org/10.1016/j.jmb.2007.05.022

Kuznetsova, I., Stepanenko, O. V., Turoverov, K. K., Zhu, L., Zhou, J. M., Fink, A. L., & Uversky, V. N. (2002). Unraveling multistate unfolding of rabbit muscle creatine kinase. *Biochimica et Biophysica Acta, 1596*, 138–155. https://doi.org/10.1016/s0167-4838(02)00212-1

Laskowski, R. A. (2009). PDBsum new things. *Nucleic Acids Research, 37*, D355–D359. https://doi.org/10.1093/nar/gkn860

Ma, X., Wang, W., Zou, M., Ding, T., Yea, X., & Liu, D. (2015). Properties and structures of commercial polygalacturonase with ultrasound treatment: Role of ultrasound in enzyme activation. *RSC Advances, 5*, 107591. https://doi.org/10.1039/C5RA19425C

Nistor, O. N., Stănciuc, N., Aprodu, I., & Botez, E. (2014). New insights into heat induced structural changes of pectin methylesterase on fluorescence spectroscopy and molecular modeling basis. *Spectrochimica Acta Part A: Molecular and Biomolecular Spectroscopy, 128*, 15–21. https://doi.org/10.1016/j.saa.2014.02.146

Pellicer, J. A., Navarro, P., & Gómez-López, V. M. (2019). Pulsed light inactivation of polygalacturonase. *Food Chemistry, 271*, 109–113. https://doi.org/10.1016/j.foodchem.2018.07.194

van Pouderoyen, G., Snijder, H. J., Benen, J. A., & Dijkstra, B. W. (2003). Structural insights into the processivity of endopolygalacturonase I from *Aspergillus niger*. *FEBS Letters, 554*(3), 462–466. https://doi.org/10.1016/S0014-5793(03)01221-3

Royer, C. A., & Weber, G. (1986). Dissociation of the lactose repressor protein tetramer using high hydrostatic pressure. *Biochemistry, 25*, 8308–8315. https://doi.org/10.1021/bi00373a027

Siddique, M. A. B., Maresca, P., Pataro, G., & Ferrari, G. (2017). Influence of pulsed light treatment on the aggregation of whey protein isolate. *Food Research International, 99*, 419–425. https://doi.org/10.1016/j.foodres.2017.06.003

van der Spoel, D., Lindahl, E., Hess, B., Groenhof, G., Mark, A. E., & Berendsen, H. J. C. (2015). GROMACS: Fast, flexible and free. *Journal of Comparative Chemistry, 26*, 1701–1719. https://doi.org/10.1002/jcc.20291

Stănciuc, N., Aprodu, I., Ioniță, E., Bahrim, G., & Râpeanu, G. (2015). Exploring the process–structure–function relationship of horseradish peroxidase through investigation of pH- and heat induced conformational changes. *Spectrochimica Acta Part A: Molecular and Biomolecular Spectroscopy, 147*, 43–50. https://doi.org/10.1016/j.saa.2015.03.023

Turoverov, K. K., Haitlina, S. Y., & Pinaev, G. P. (1976). Ultra-violet fluorescence of actin. Determination of native actin content in actin preparations. *FEBS Letters, 62*, 4–6. https://doi.org/10.1016/0014-5793(76)80003-8

Van Santen, Y., Benen, J. A., Schröter, K. H., Kalk, K. H., Armand, S., Visser, J., & Dijkstra, B. W. (1999). 1.68-A crystal structure of endopolygalacturonase II from *Aspergillus niger* and identification of active site residues by site-directed mutagenesis. *Journal of Biological Chemistry, 274*(43), 30474–30480. https://doi.org/10.1074/jbc.274.43.30474